

# Clean grain boundaries and weak links in high $T_c$ superconducting $\text{YBa}_2\text{Cu}_3\text{O}_{7-x}$ thin films

D. H. Shin, J. Silcox, S. E. Russek, D. K. Lathrop, B. Moeckly, and R. A. Buhrman  
*School of Applied and Engineering Physics, Cornell University, Ithaca, New York 14853*

(Received 8 January 1990; accepted for publication 16 May 1990)

It is demonstrated that polycrystalline thin films of high  $T_c$  superconducting  $\text{YBa}_2\text{Cu}_3\text{O}_{7-x}$  can be grown with clean grain boundaries, i.e., without a boundary layer of segregation or different phase. In clean stoichiometric samples, angular misorientations of grains may be the origin of weak link behavior. High-resolution scanning transmission electron microscope images of films grown on  $\text{ZrO}_2$  and  $\text{MgO}$  by reactive evaporation, reactive sputtering, and laser ablation show atomic lattice images of clean grain boundaries. X-ray microanalysis with a 10 Å spatial resolution also indicates no composition deviation at the grain boundaries. Grain sizes and epitaxial relations of samples prepared by different methods are characterized.

Highly  $c$ -oriented epitaxial films of superconducting  $\text{YBa}_2\text{Cu}_3\text{O}_{7-x}$  have been grown *in situ* by a number of different techniques on a number of different substrates.<sup>1-3</sup> These films show critical current densities ( $J_c$ 's)  $\sim 2$ – $3$  orders of magnitudes larger than those of the bulk high  $T_c$  samples.<sup>4,5</sup> Random orientations of grains in bulk samples coupled with disordered, nonstoichiometric regions at the grain boundaries are thought to cause weak Josephson coupling between grains and lead to suppressed  $J_c$ 's.<sup>6-8</sup> In thin films, it is thought that the grain boundaries are clean and highly oriented and that this leads to an overall increase in the  $J_c$ 's. In this letter, we present high-resolution scanning transmission electron microscope (STEM) images as evidence that most grain boundaries in thin-film  $\text{YBa}_2\text{Cu}_3\text{O}_{7-x}$  superconductors grown by reactive evaporation, reactive sputtering, and laser ablation are clean. This conclusion is reinforced by high spatial resolution x-ray microanalysis. On substrates with a large lattice mismatch, we have observed several characteristic grain orientations which lead to tilt boundaries whose presence correlates with the presence of weak links in transport measurements.

Thin films of high  $T_c$  superconducting  $\text{YBa}_2\text{Cu}_3\text{O}_{7-x}$  were grown *in situ* by reactive evaporation, reactive sputtering, and laser ablation on  $\text{MgO}$  and  $\text{ZrO}_2$  substrates. Details of the film growth methods have been described elsewhere.<sup>1,2,9</sup> Films of about 3000 Å in thickness were grown in oxygen partial pressures ranging from  $5 \times 10^{-4}$  Torr for evaporation to 0.4 Torr for laser ablation and at substrate temperatures of 650–750 °C. Typical  $T_c$ 's for these films range between 75 and 90 K with critical current densities of 1 to  $15 \times 10^6$  A/cm<sup>2</sup> at 4.2 K. The best films were made by laser ablation and have  $J_c$ 's of  $\sim 10^6$  A/cm<sup>2</sup> at 77 K.

Thinning of specimens for electron transmission has been done by mechanical polishing followed by argon ion milling. The specimen was thinned at room temperature until a small hole began to appear, then the ion voltage was lowered from 6 to 3 kV in order to minimize the surface damage on the specimen.<sup>10</sup> The specimens were then studied with a VG HB501A scanning transmission electron

microscope (STEM) operating at 100 kV. This STEM has a demonstrated resolution of better than 2 Å in both annular dark field (with  $C_s = 1.2$  mm)<sup>11</sup> and bright field (with  $C_s = 0.7$  mm)<sup>12</sup> imaging modes.

In the laser-ablated samples, we find that the films are almost entirely  $c$  oriented. Figure 1(a) is a high-resolution STEM bright field image of a small angle twist boundary in a  $c$ -axis oriented film grown by laser ablation on a (100)  $\text{MgO}$  substrate at a substrate temperature of 650 °C. The grains in this image have nearly the same orientation, which is a result of identical epitaxial orientations in their nucleation stage. There is a possibility of 90° rotation, i.e., the exchange of  $a$  and  $b$  axes, which is not distinguishable from the STEM images. It is evident from the lattice image that the crystalline structure of the 1-2-3 phase extends up to the grain boundary. Boundaries of this type will be designated 0° boundaries in the rest of this paper. Figure 1(b) shows a similarly clean grain boundary. The grain boundary in Fig. 1(b) is a tilt boundary with tilt angle of  $\sim 8^\circ$ .

A number of energy dispersive x-ray (EDX) profiles have been taken across the grain boundaries of various types with an electron probe diameter  $< 10$  Å. Figure 2 shows a typical atomic concentration profile of yttrium, barium, and copper in a film grown on zirconia by reactive evaporation. No significant change of composition is observed at the grain boundaries.

Note that the tilt angles are not the result of randomly oriented neighboring grains. Unlike the  $\text{SrTiO}_3/\text{YBa}_2\text{Cu}_3\text{O}_{7-x}$  system, the  $\text{MgO}/\text{YBa}_2\text{Cu}_3\text{O}_{7-x}$  system, for example, has a large lattice mismatch of 8–9% along the [100] direction, and therefore, the grains do not all nucleate along the [100] direction of  $\text{MgO}$ . For example, the [100] of high  $T_c$  grains can line up with the [110] of  $\text{MgO}$  with 2.8% mismatch, or either the [210] or the [310] of the high  $T_c$  can be aligned along the [100] of  $\text{MgO}$  with 2.5% or 3.4% mismatch, respectively. These orientations make angles of 45°, 26.6°, and 18.4°, respectively, between the [100] of the substrate and the [100] of high  $T_c$ , and can result in grain boundary tilt angles of 8.2°, 18.4°, 26.6°, 36.8°, and 45° (Not considering 90° rotation, i.e., exchange of  $a$  and  $b$  axes). Although the degree of mismatch can be

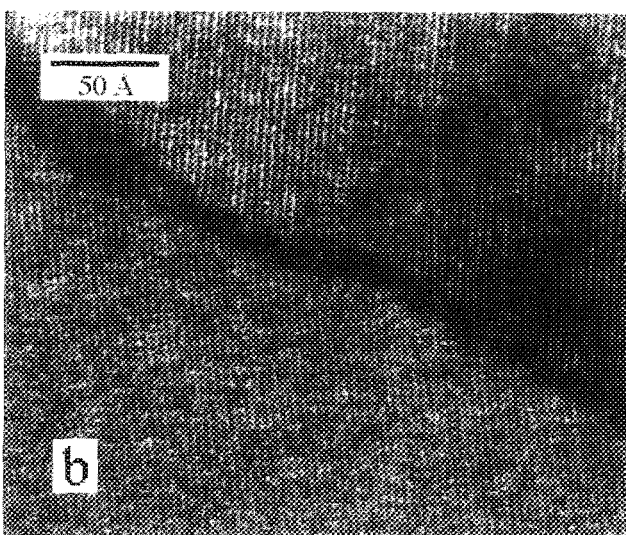
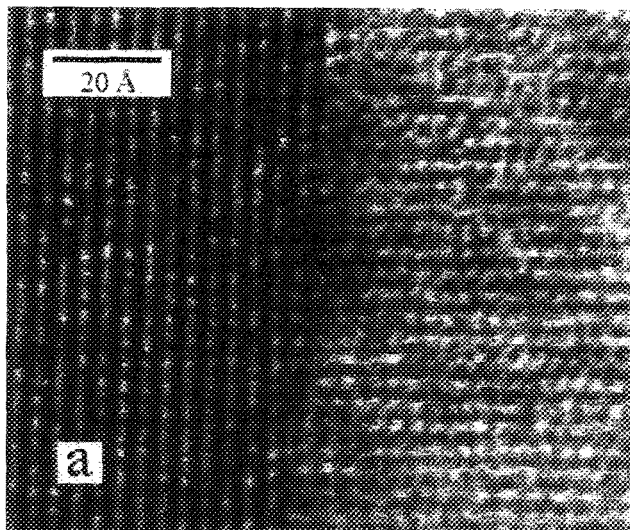


FIG. 1. High-resolution STEM bright field images of grain boundaries in  $c$ -axis oriented  $\text{YBa}_2\text{Cu}_3\text{O}_{7-x}$  films. Films were grown by laser ablation on MgO substrates. Grain boundary tilt angles in (a) and (b) are  $\sim 0^\circ$ ,  $\sim 8^\circ$ , respectively.

considerably reduced by these noncommensurate lattice matches, it is difficult to predict which orientation will be favored since the actual nucleation of the film will depend on the detailed oxygen sublattice configuration in the particular orientation.<sup>13</sup> It is observed that, as the growth temperature is increased to  $\sim 670^\circ\text{C}$ , the film grown on heat-

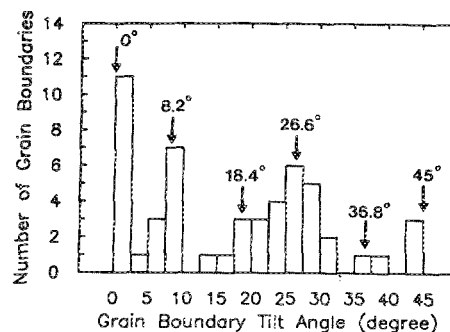


FIG. 3. Histogram showing the grain boundary tilt angle distribution in high  $T_c$   $\text{YBa}_2\text{Cu}_3\text{O}_{7-x}$  films grown on (100) MgO. Samples were grown either by laser ablation ( $T_s = 650^\circ\text{C}$ ) or by reactive sputtering ( $T_s = 680^\circ\text{C}$ ).

treated MgO tends to have large epitaxial grains  $\geq 1 \mu\text{m}$  with 1–2% of  $a$ -axis oriented inclusions and very small randomly oriented  $c$ -axis inclusions. Since there are fewer high angle boundaries, weak links do not show up in typical  $I$ - $V$  measurements from samples grown at higher temperatures.

Figure 3 is a histogram showing the number of observed grain boundaries with certain tilt angles in samples grown on the MgO substrate either by laser ablation ( $T_s = 650^\circ\text{C}$ ) or by sputtering ( $T_s = 680^\circ\text{C}$ ). The angles have been directly measured from the STEM images. Since  $0^\circ$  boundaries are often difficult to recognize as grain boundaries, the actual frequency of  $0^\circ$  boundaries may be considerably higher. Although the distribution is not sharply peaked at those angles, it suggests the existence of several preferred epitaxial orientations. The broad distribution around the peaks is due to small angle deviations from the preferred orientations due to the imperfect lattice match.

X-ray diffraction pole figure studies on similar films ( $T_s = 650^\circ\text{C}$ ) show that the grains have predominantly a  $0^\circ$  orientation, i.e.,  $[100]\text{MgO}$  is parallel to  $[100]\text{YBa}_2\text{Cu}_3\text{O}_{7-x}$  with small amounts (1–20%) of misoriented grains for films on MgO and only  $0^\circ$  orientation for films on  $\text{SrTiO}_3$ . The degree of orientation on MgO substrates can be varied by varying the MgO surface preparation and growth conditions.<sup>9</sup>

These clean, but large angle, grain boundaries may play an important role in the transport properties of these films. Transport measurements on  $\sim 1\text{-}\mu\text{m}$ -wide lines lithographically patterned in similar laser-ablated films grown on MgO indicate the existence of weak links with quasi-Josephson-like properties, while films grown on  $\text{SrTiO}_3$  do not.<sup>9</sup> Critical current densities for narrow lines can vary by two orders of magnitude depending on whether or not there is a weak link in the line. Since the  $\text{SrTiO}_3/\text{YBa}_2\text{Cu}_3\text{O}_{7-x}$  system has a very small lattice mismatch, the grains in the film grown on  $\text{SrTiO}_3$  are more likely to be aligned along the  $[100]$  of the substrate, and therefore, large angle grain boundaries are much less likely to be observed.<sup>14,15</sup> This implies that the weak link may be due either to the large angle grain boundary or to the misoriented grain as a whole.

Grain sizes have been measured for films grown by the

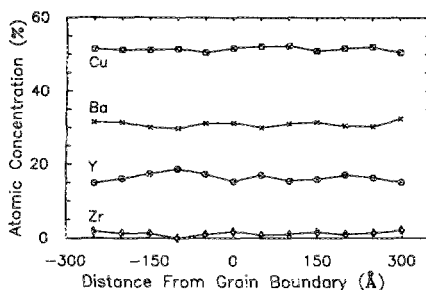


FIG. 2. EDX profile of atomic concentrations across the grain boundary in  $\text{YBa}_2\text{Cu}_3\text{O}_{7-x}$  film grown on (100)  $\text{ZrO}_2$  by reactive evaporation.

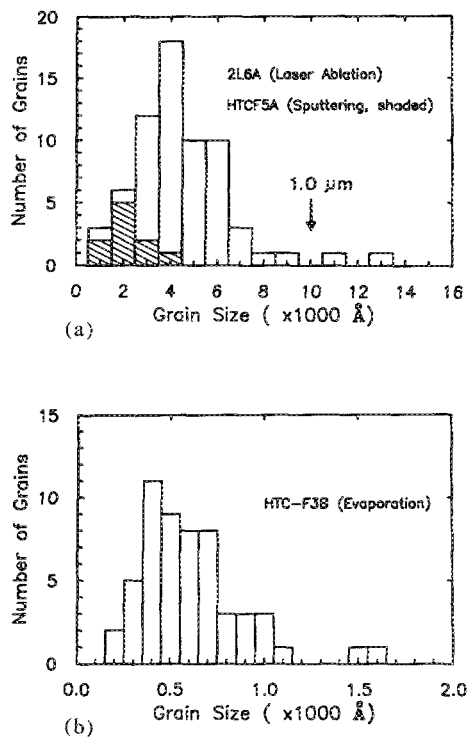


FIG. 4. Histogram showing the grain size distribution in (a) films grown by laser ablation ( $T_s = 650^\circ\text{C}$ ) and by reactive sputtering ( $T_s = 680^\circ\text{C}$ ), and (b) films grown by reactive evaporation ( $T_s = 750^\circ\text{C}$ ). The arrow marked  $1 \mu\text{m}$  indicates the scale of lithographic lines in which weak link behavior has been observed.

three different methods. Figure 4(a) shows the grain size distribution in films grown on MgO by laser ablation ( $T_s = 650^\circ\text{C}$ ) and by reactive sputtering ( $T_s = 680^\circ\text{C}$ ), and Fig. 4 (b) shows the grain size distribution in a film grown on  $\text{ZrO}_2$  by reactive evaporation ( $T_s = 750^\circ\text{C}$ ). The average grain size increases from  $610 \text{ \AA}$  for the evaporated film to  $2300 \text{ \AA}$  for the sputtered film and to  $4500 \text{ \AA}$  for the laser-ablated film despite the decrease in growth temperatures. The growth temperatures ( $T_s$ 's) of these films are characteristic of the optimum growth temperature for each deposition process. More than 70% of the film area is covered by grains larger than the average grain size and these large grains may dominate transport properties. The large

grain size of laser-ablated films accounts for the ability to isolate single Josephson weak links in  $\sim 1\text{-}\mu\text{m}$ -wide lines.

In summary, high quality, near stoichiometric films of  $\text{YBa}_2\text{Cu}_3\text{O}_{7-x}$  with large  $J_c$  have been grown *in situ* by reactive evaporation, reactive sputtering, and laser ablation. High-resolution STEM images of grain boundaries in *c*-oriented films indicate that the grain boundaries are mostly clean and free of second phase or segregation. High angle grain boundaries, which might be responsible for the weak links, have been identified as resulting from a number of possible epitaxial orientations of nucleation of grains on the substrate.

The authors would like to thank P. Xu, R. Loane, and Dr. E. J. Kirkland for helpful discussions. This work was supported by DARPA (grant No. 88-K-0374). The UHV-STEM was acquired through the NSF (DMR-8314255) and Cornell University, and is operated through the Cornell Material Science Center (NSF DMR-8516616).

- <sup>1</sup>D. K. Lathrop, S. E. Russek, and R. A. Buhrman, *Appl. Phys. Lett.* **51**, 1554 (1987).
- <sup>2</sup>D. K. Lathrop, S. E. Russek, K. Tanabe, and R. A. Buhrman, *IEEE Trans. Magn.* **25**, 2218 (1989).
- <sup>3</sup>X. D. Wu, D. Dijkamp, S. B. Ogale, A. Inam, E. W. Chase, P. F. Miceli, C. C. Chang, J. M. Tarascon, and T. Venkatesan, *Appl. Phys. Lett.* **51**, 861 (1987).
- <sup>4</sup>P. Chaudhari, R. H. Koch, R. B. Laibowitz, T. R. McGuire, and R. J. Gambino, *Phys. Rev. Lett.* **58**, 2684 (1987).
- <sup>5</sup>S. Jin, T. H. Tiefel, R. C. Sherwood, M. E. Davis, R. B. van Dover, G. W. Kammlott, R. A. Fastnacht, and H. D. Keith, *Appl. Phys. Lett.* **52**, 2074 (1988).
- <sup>6</sup>T. L. Hylton, A. Kapitulnik, M. R. Beasley, J. P. Carini, L. Drabek, and G. Gruner, *Appl. Phys. Lett.* **53**, 1343 (1988).
- <sup>7</sup>J. W. Ekin, A. I. Braginski, A. J. Panson, M. A. Janocko, D. W. Capone, II, N. J. Zaluzec, B. Flandermeyer, O. F. de Lima, M. Hong, J. Kwo, and S. H. Kiou, *J. Appl. Phys.* **62**, 4821 (1987).
- <sup>8</sup>D. Dimos, P. Chaudhari, J. Mannhart, and F. K. LeGoues, *Phys. Rev. Lett.* **61**, 219 (1988).
- <sup>9</sup>B. Moeckly, D. K. Lathrop, G. Redinbo, S. E. Russek, and R. A. Buhrman, to be published in *Materials Research Society Symposium Proceedings*, Materials Research Society, Pittsburgh, PA, 1990.
- <sup>10</sup>C. H. Chen, H. S. Chen, and S. H. Liou, *Appl. Phys. Lett.* **53**, 2339 (1988).
- <sup>11</sup>D. H. Shin, E. J. Kirkland, and J. Silcox, *Appl. Phys. Lett.* **55**, 2456 (1989).
- <sup>12</sup>P. Xu, E. J. Kirkland, J. Silcox, and R. Keyse, to be published in *Ultramicroscopy* **32**, 93 (1990).
- <sup>13</sup>M. G. Norton, L. A. Tietz, S. R. Summerfelt, and C. B. Carter, *Appl. Phys. Lett.* **55**, 2348 (1989).
- <sup>14</sup>D. M. Hwang, L. Nazar, T. Venkatesan, and X. D. Wu, *Appl. Phys. Lett.* **52**, 1834 (1988).
- <sup>15</sup>C. H. Chen, J. Kwo, and M. Hong, *Appl. Phys. Lett.* **52**, 841 (1988).